Regular Article

blood

THROMBOSIS AND HEMOSTASIS

Disulfide HMGB1 derived from platelets coordinates venous thrombosis in mice

Konstantin Stark,[1,2] Vanessa Philippi,[1] Sven Stockhausen,[1] Johanna Busse,[1] Antonella Antonelli,[3] Meike Miller,[1] Irene Schubert,[1] Parandis Hoseinpour,[1] Sue Chandraratne,[1] Marie-Luise von Brühl,[1] Florian Gaertner,[1,2] Michael Lorenz,[1] Alessandra Agresti,[3] Raffaele Coletti,[1] Daniel J. Antoine,[4] Ralf Heermann,[5] Kirsten Jung,[5] Sven Reese,[6] Iina Laitinen,[7] Markus Schwaiger,[7] Axel Walch,[8] Markus Sperandio,[2,9] Peter P. Nawroth,[10] Christoph Reinhardt,[11,12] Sven Jäckel,[11,12] Marco E. Bianchi,[3,*] and Steffen Massberg[1,2,*]

[1]Medizinische Klinik I, Ludwig-Maximilians-Universität, Munich, Germany; [2]German Centre for Cardiovascular Research, Partner Site Munich Heart Alliance, Munich, Germany; [3]Chromatin Dynamics Unit, San Raffaele University and Scientific Institute, Milan, Italy; [4]Medical Research Council Center for Drug Safety Science, Department of Molecular and Clinical Pharmacology, University of Liverpool, Liverpool, United Kingdom; [5]Munich Center for Integrated Protein Science, Department of Biology I, and [6]Lehrstuhl für Anatomie, Histologie und Embryologie, Faculty of Veterinary Medicine, Ludwig-Maximilians Universität, Munich, Germany; [7]Nuklearmedizinische Klinik und Poliklinik, Klinikum rechts der Isar, Technische Universität München, Munich, Germany; [8]Helmholtz Zentrum München, Deutsches Forschungszentrum für Umwelt und Gesundheit, Institut für Pathologie, Neuherberg, Germany; [9]Walter Brendel Centre of Experimental Medicine, Ludwig-Maximilians-Universität, Munich, Germany; [10]Department of Internal Medicine I and Clinical Chemistry, University of Heidelberg, Heidelberg, Germany; [11]Center for Thrombosis and Hemostasis University Medical Center Mainz, Mainz, Germany; and [12]German Center for Cardiovascular Research, Partner Site RheinMain, Mainz, Germany

Key Points

- Sterile inflammation inducing venous thrombosis is coordinated by the damage-associated molecular pattern HMGB1 delivered by platelets.
- The effect of HMGB1 depends on the redox form, and disulfide HMGB1 induces NET formation, platelet aggregation, and monocyte activation.

Deep venous thrombosis (DVT) is one of the most common cardiovascular diseases, but its pathophysiology remains incompletely understood. Although sterile inflammation has recently been shown to boost coagulation during DVT, the underlying molecular mechanisms are not fully resolved, which could potentially identify new anti-inflammatory approaches to prophylaxis and therapy of DVT. Using a mouse model of venous thrombosis induced by flow reduction in the vena cava inferior, we identified blood-derived high-mobility group box 1 protein (HMGB1), a prototypical mediator of sterile inflammation, to be a master regulator of the prothrombotic cascade involving platelets and myeloid leukocytes fostering occlusive DVT formation. Transfer of platelets into *Hmgb1*$^{-/-}$ chimeras showed that this cell type is the major source of HMGB1, exposing reduced HMGB1 on their surface upon activation thereby enhancing the recruitment of monocytes. Activated leukocytes in turn support oxidation of HMGB1 unleashing its prothrombotic activity and promoting platelet aggregation. This potentiates the amount of HMGB1 and further nurtures the accumulation and activation of monocytes through receptor for advanced glycation end products (RAGE) and Toll-like receptor 2, leading to local delivery of monocyte-derived tissue factor and cytokines. Moreover, disulfide HMGB1 facilitates formation of prothrombotic neutrophil extracellular traps (NETs) mediated by RAGE, exposing additional HMGB1 on their extracellular DNA strands. Eventually, a vicious circle of coagulation and inflammation is set in motion leading to obstructive DVT formation. Therefore, platelet-derived disulfide HMGB1 is a central mediator of the sterile inflammatory process in venous thrombosis and could be an attractive target for an anti-inflammatory approach for DVT prophylaxis. (*Blood*. 2016; 128(20):2435-2449)

Introduction

Deep venous thrombosis (DVT) and its major complication, venous thromboembolism, constitute major health care issues associated with substantial morbidity and mortality. Despite the effort to identify risk factors and to develop new preventive strategies, the incidence of DVT is increasing.[1] Prevention of DVT in hospitalized patients is usually achieved by anticoagulation, for example, using heparins or more recently by non-vitamin K oral anticoagulants. However, anticoagulants carry along an increased risk of bleeding due to impaired hemostasis; hence, prevention of DVT without compromising the hemostatic system would be preferable. Recently, we and others have shown that DVT has to be considered an aberrant sterile inflammatory process, where innate immunity drives clot formation.[2-7] In particular, monocytes and neutrophils support coagulation during DVT by delivering tissue factor (TF), the activator of the extrinsic

Submitted 13 April 2016; accepted 12 August 2016. Prepublished online as *Blood* First Edition paper, 29 August 2016; DOI 10.1182/blood-2016-04-710632.

*M.E.B. and S.M. share senior authorship.

The online version of this article contains a data supplement.

There is an Inside *Blood* Commentary on this article in this issue.

The publication costs of this article were defrayed in part by page charge payment. Therefore, and solely to indicate this fact, this article is hereby marked "advertisement" in accordance with 18 USC section 1734.

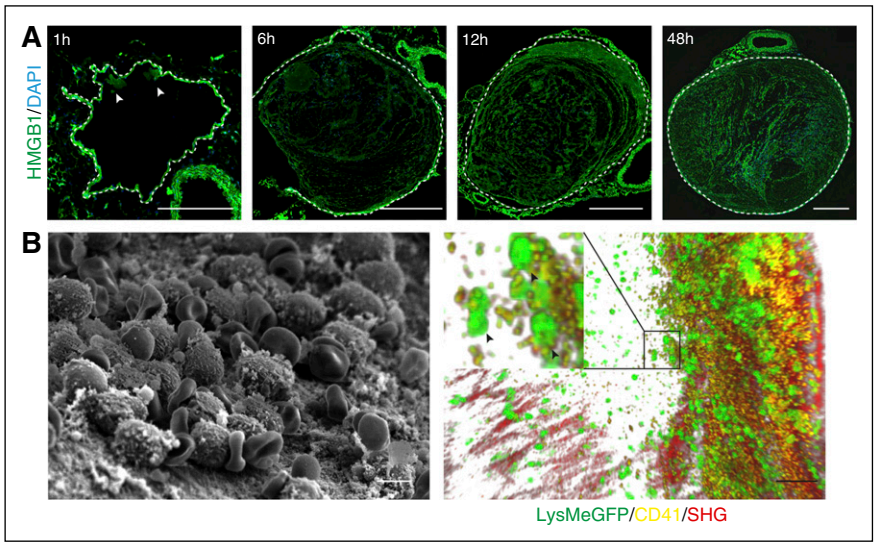

Figure 1. Presence of HMGB1 in the developing venous thrombus. (A) Immunofluorescence staining of cross sections of the IVC for HMGB1 (green) and DAPI (blue) 1, 6, 12, and 48 hours after flow reduction. Arrowheads show HMGB1 deposition, dotted line indicates endothelium; bar, 200 μm. (B) Left, Scanning electron microscopy of the IVC 6 hours after flow reduction, showing the intact endothelium covered by cell aggregates and fibrin; bar, 5 μm. Right, Three-dimensional reconstruction of images from intravital 2-photon microscopy showing the vessel wall (second harmonic generation, red), with adherent platelets (yellow) and neutrophils (green); bar, 50 μm. Box, Platelet-myeloid leukocyte aggregates indicated by arrowheads at higher magnification. (A-B) Images representative of n = 3 experiments.

coagulation pathway, and through the formation of neutrophil extracellular traps (NETs), negatively charged DNA structures that activate coagulation and platelets.[2-7] However, how exactly the sterile inflammatory process is initiated and maintained during DVT remains incompletely understood.[8]

Sterile inflammation is characterized by an immune response in the absence of pathogenic organisms where cell death leads to the release of danger-associated molecular patterns (DAMPs).[9] Once in the extracellular space, DAMPs elicit a strong immune response that serves to remove dead cells, but may result in additional damage due to inflammatory off-target effects.[10] Not only can necrosis lead to the release of DAMPs, but immune cells as well as platelets can also actively release these mediators.[11-13] High-mobility group box 1 (HMGB1), a nuclear protein attached to DNA which stabilizes nucleosome formation and is involved in the regulation of gene expression, is one of the prototypical DAMPs.[14] Once released into the extracellular space, HMGB1 elicits and fine-tunes leukocyte recruitment and activation. HMGB1 functionality depends on the redox state of the protein: whereas the reduced form primarily serves as a chemoattractant, the oxidized intermediate induces leukocyte activation and release of proinflammatory cytokines; these effects are lost in the terminally oxidized sulfonyl form.[15,16] In addition, HMGB1 has recently been reported to induce platelet aggregation in vitro and in vivo in the setting of microvascular thrombosis.[17,18] However, whether and how different HMGB1 redox forms contribute to sterile inflammation and clot formation during macrovascular DVT remains elusive.

Here, we used a mouse model of flow reduction in the inferior vena cava (IVC) to identify a novel function of HMGB1 in coordinating macrovascular venous thrombosis.[6,19] We show that blood cells, particularly platelets, deposit reduced HMGB1 on the luminal aspect of venous endothelial cells early in the process of DVT formation. Pharmacological inhibition or loss of blood-derived HMGB1 prevents DVT formation. Platelet-derived HMGB1 propagates DVT by operating at least 3 different mechanisms: (1) by triggering monocyte recruitment and supporting monocyte TF production; (2) by facilitating the formation of prothrombotic NETs providing additional HMGB1, and (3) by increasing platelet accumulation and aggregation. These effects of HMGB1 involve receptor for advanced glycation end products (RAGE), Toll-like receptor 2/4 (TLR2/4), and depend on the redox status of the protein. Hence, we identify HMGB1 as a promising new target in the sterile inflammatory response, which eventually activates the coagulation system and triggers DVT.

Methods

Animals

C57BL/6, Balb/c, *Myd88*$^{-/-}$, and *Tlr4*$^{-/-}$ mice were obtained from The Jackson Laboratory or Janvier (Balb/c) and generated as described.[20,21] *Tlr2*$^{-/-}$ mice were generated as described.[22] *Rage*$^{-/-}$ mice were provided by P.P.N.[23] C57BL/6 mice were used as control for *Myd88*$^{-/-}$, *Tlr2*$^{-/-}$, *Rage*$^{-/-}$, and *Tlr4*$^{-/-}$ mice, which have been backcrossed to a C57Bl/6 background for at least 7 generations. *Hmgb1*$^{-/-}$ chimeras were generated as described from heterozygous crossings, and fetal liver cells of *Hmgb1*$^{-/-}$ and *Hmgb1*$^{+/+}$ siblings were injected into Balb/c mice for generation of chimeras.[24] Heterozygous LysM$^{eGFP/+}$ and CX3CR1$^{GFP/+}$ knock-in mice were generated as described.[25,26] All procedures performed on mice were approved by the local legislation on protection of animals (Regierung von Oberbayern, Munich, Germany). HMGB1-deficient mice were maintained in Ospedale San Raffaele, under protocols reviewed and approved by the Animal Care and Use Committee of Ospedale San Raffaele and by the Ministry of Health of Italy.

Mouse model of flow restriction in the IVC

After a median laparotomy, the IVC was exposed and a space holder was positioned followed by a narrowing ligature. Subsequently, the wire was removed to avoid complete vessel occlusion. Side branches were not ligated or manipulated. All groups were age, sex, and weight matched. Mice with bleedings or any injury of the IVC during surgery were excluded from further analysis. BoxA (500 μg; HMGBiotech) was administered IV into the tail vein of Balb/c mice before surgery; phosphate-buffered saline (PBS) was used as control. Anakinra (1 mg/kg) was given subcutaneously (s.c.) 1 hour before flow reduction and then every 24 hours into C57Bl/6 mice; NaCl was used as control. 3S- and disulfide HMGB1 were injected IV at 0.5 mg/kg immediately before the surgery and 24 hours afterward into *Hmgb1*$^{-/-}$ chimeras. For nuclear staining, propidium iodide 10 mg/kg body weight was injected IV 30 minutes before the mice were sacrificed. For thrombus weight measurement after 48 hours, the IVC was excised just below the renal veins and proximal to the confluence of the common iliac veins.

Intravital epifluorescence microscopy

Murine platelets were isolated from whole blood and labeled with Rhodamine B.[27] For quantification of leukocyte adhesion, acridine orange (Sigma-Aldrich)

was injected IV or CX3CR1$^{GFP/+}$ mice were used. Imaging was performed with an Olympus BX51WI microscope using a 20× (NA 0.95) water-immersion objective and an ORCA-ER CCD camera (Hamamatsu).

Intravital 2-photon microscopy

A TrimScope (LaVision Biotech) connected to an upright Olympus microscope was used, equipped with a MaiTai laser (Spectra-Physics) and a 20× water-immersion objective (numerical aperture 0.95; Olympus). LysM$^{eGFP/+}$ mice and platelets labeled with Cell Tracker violet (Invitrogen) were used.

Ultrasound

Ultrasound examinations were performed using the MyLab One VET system (Esaote SpA) adapted to a SL 3116 linear probe of 15 to 22 MHz.

Computed tomography

Mice were imaged with the Inveon small animal positron emission tomography/computed tomography (CT) scanner (Siemens). As contrast agent, 0.1 mL of eXIA 160-XL (Binitio Biomedical Inc) was injected IV. CT projections were acquired as described previously (exposure time of 400 ms, x-ray voltage 80 kVp, anode current 400 μA for a full 360° rotation).[6]

Generation of fetal liver cell chimeras

For generation of fetal liver chimeras, 6×10^6 fetal liver cells of *Hmgb1*$^{+/+}$ and *Hmgb1*$^{-/-}$ animals were injected into the tail vein of irradiated (650 rad) Balb/c mice. Six to eight weeks after transplantation, thrombus formation was induced.

Transfusion of platelets and neutrophils

Platelets were isolated from Balb/c mice or *Hmgb1*$^{-/-}$ chimeras and 150 000 were injected into the tail vein before the flow reduction of the IVC was performed. Neutrophils were isolated from the bone marrow of Balb/c mice by differential gradient centrifugation using an isotonic discontinuous Percoll gradient (72%/64%/52%) at 4°C; Ly6G$^+$ cells were >90% as determined by fluorescence-activated cell sorting. Neutrophils (2×10^6) were injected into the tail vein before surgery.

Immunofluorescence staining of frozen sections

The IVC was embedded in optimal cutting temperature compound, frozen at −80°C, and was cut with a cryotome (CryoStar NX70 Kryostat; ThermoFisher Scientific) into 4-μm sections. Specimens were fixed with 4% formaldehyde and blocked with the respective serum. The sections were incubated with primary antibodies for CD41 (MWReg30, BD Biosciences; isotype: rat immunoglobulin G1 [IgG1], Abcam), Ly6G (clone 1A8, BD Biosciences; isotype: rat IgG2a, eBioscience), myeloperoxidase (MPO) (rabbit polyclonal, DAKO; isotype: rabbit immunoglobulin fraction, DAKO), F4/80 (clone Cl:A3-1, AbD Serotec; isotype: rat IgG2b, eBioscience), and HMGB1 (rabbit polyclonal, Abcam; isotype: rabbit immunoglobulin fraction, DAKO). Next, Alexa-conjugated secondary antibodies (Invitrogen) were used for detection. DNA was stained with 4′,6-diamidino-2-phenylindole (DAPI) (Invitrogen). Images were acquired using a Zeiss Axio imager microscope with an AxioCam. For quantification of NET formation 3 distinct parameters had to be met: (1) extracellular DNA protrusions had to be present, (2) the protrusion had to originate from cells staining positive for Ly6G, and (3) the structures had to be decorated with MPO. Only if all of these criteria were fulfilled could a structure be defined as NET and be included into the quantification.

Scanning electron microscopy

The IVC was perfused with PBS, followed by perfusion fixation with 1% phosphate-buffered glutaraldehyde. The veins were mounted with carbon paint, sputter-coated with platinum, and examined using a field emission scanning electron microscope (JSM-6300F; Jeol Ltd).[28]

SPR spectroscopy and Interaction Map analysis

Surface plasmon resonance (SPR) assays were performed at 25°C in a Biacore T200 using carboxymethyl dextran sensor chips (CM5 Sensor Chip Series S; GE Healthcare) in HBS-EP+ buffer (GE Healthcare). First, the chips were equilibrated with HBS-EP+ buffer until the dextran matrix had swollen. Then, the chips were coated with anti-His antibodies (Biacore His-capture kit; GE Healthcare), so that the chip surface allows for complete regeneration of His-tagged molecules from a sensor chip. Then, 2 of the 4 flow cells on each sensor chip were activated by injecting a 1:1 mixture of N-ethyl-N-(3-dimethylaminopropyl) carbodiimide hydrochloride and N-hydroxysuccinimide using the standard amine-coupling protocol. Both flow cells were then loaded with a final concentration of 50 μg/mL anti-His antibody in 10 mM acetate (pH 4.5) using a contact time of 420 seconds so that the surfaces contained antibody densities equivalent to ~14 000 resonance units (RU). Free binding sites on the flow cells were saturated by injection of 1 M ethanolamine/HCl (pH 8.0). Preparation of chip surfaces was carried out at a flow rate of 10 μL per minute. Analyses of interaction between RAGE-His and the 3 HMBG1 derivatives were performed in HBS-EP+ buffer. First, 20 μg/mL mouse RAGE-His (Sino Biological Inc) was captured onto the second flow cell using a contact time of 60 seconds at a constant flow rate of 10 μL per minute, followed by a stabilization time of 10 seconds so that ~1000 RU of RAGE-His were captured. Then, increasing concentrations (1, 10, 25, 50 nM, 2× 100 nM, 250, 500, 1000, and 2000 nM) of nonoxidizable 3S-HMBG1, disulfide HMBG1, and sulfonyl HMGB1 (HMGBiotech) were injected over both flow cells using a contact time of 180 seconds each and a final dissociation step of 600 seconds at a flow rate of 30 μL per minute. After each cycle, the chip was regenerated by injection of 10 mM glycine (pH 1.5) for 60 seconds at a flow rate of 30 μL per minute over both flow cells, which completely removed RAGE-His from the surface. Sensorgrams were recorded using Biacore T200 Control software 2.0 and analyzed with Biacore T200 Evaluation software 2.0. The surface of flow cell 1 was used to obtain blank sensorgrams for subtraction of the bulk refractive index background. The referenced sensorgrams were then normalized to a baseline of 0. Spikes in the sensorgrams at the start and the end of the injections emerged from the run-time difference between the flow cells on each chip. Interaction Map (IM) analysis was performed to differentiate independent binding events in the SPR data and calculations were performed on the Ridgeview diagnostic server (Ridgeview Diagnostics).[29] The resulting files were then evaluated for spots in the TraceDrawer 1.5 software, and the IM spots were quantified.

Mass spectrometry

Platelet-rich plasma from healthy human donors was isolated as described and, where indicated, platelets were activated group with thrombin (0.1 U/mL).[30] Platelets and supernatant were separated by centrifugation and incubated with 10 mM iodoacetamide, followed by 30 mM dithiothreitol and 90 mM N-ethylmaleimide. Platelets were lysed (RIPA lysis buffer; ThermoFisher Scientific) and stored at −80°C. Characterization of HMGB1 redox modifications were determined as described previously by tandem mass spectrometry.[31,32]

Reverse transcriptase polymerase chain reaction

Monocytes were isolated from healthy human donors (purity >90%) and incubated with different redox forms of HMGB1 and lipopolysaccharide (LPS) as positive control for 3 hours. RNA was isolated and template complementary DNA was synthesized from 2 μg of total RNA using the High Capacity cDNA Archive kit (Applied Biosystems) and applied in Sybr Green assays. The murine sequences of TF, interleukin-6 (IL-6), and IL-1β were detected by QuantiTect primer assays (Qiagen).

Whole-blood aggregometry

Platelet aggregation was analyzed using whole blood by multiplate impedance platelet aggregometry (Dynabyte) as described.[30] Blood from healthy human donors was anticoagulated with hirudin and stimulated with different redox forms of HMGB1 as indicated compared with buffer. In 1 set of experiments, anticoagulated whole blood was incubated with the different HMGB1 redox forms for 30 minutes followed by stimulation with adenosine 5′-diphosphate (ADP) (2 μM).

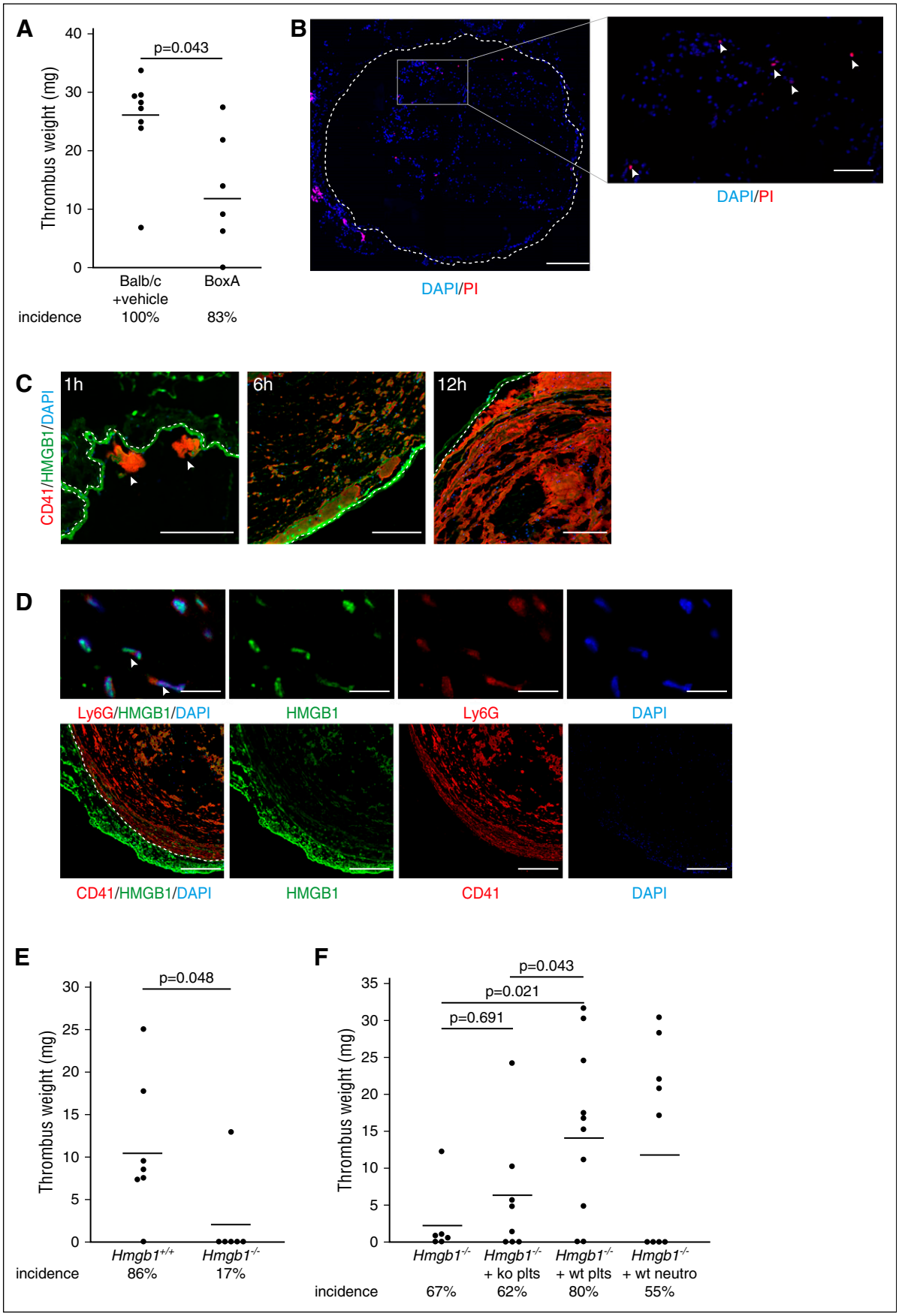

Figure 2. Blood-derived HMGB1 causes venous thrombosis. (A) Thrombus weight in Balb/c mice treated with PBS (n = 8) compared with BoxA (n = 6). (B) Left, Immunofluorescence staining of cross-sections of the IVC for propidium iodide (PI) (red) and DAPI (blue) 6 hours after flow reduction. Dotted line indicates endothelium; bar, 200 μm. Right, Higher magnification of intraluminal propidium iodide–positive cells (arrowheads); bar, 70 μm. (C) Immunofluorescence staining of cross-sections of the IVC 1, 6, and 12 hours after flow reduction for CD41 (red) and HMGB1 (green). Nuclei are counterstained with DAPI (blue). Dotted line indicates endothelium; bar, 100 μm. Images

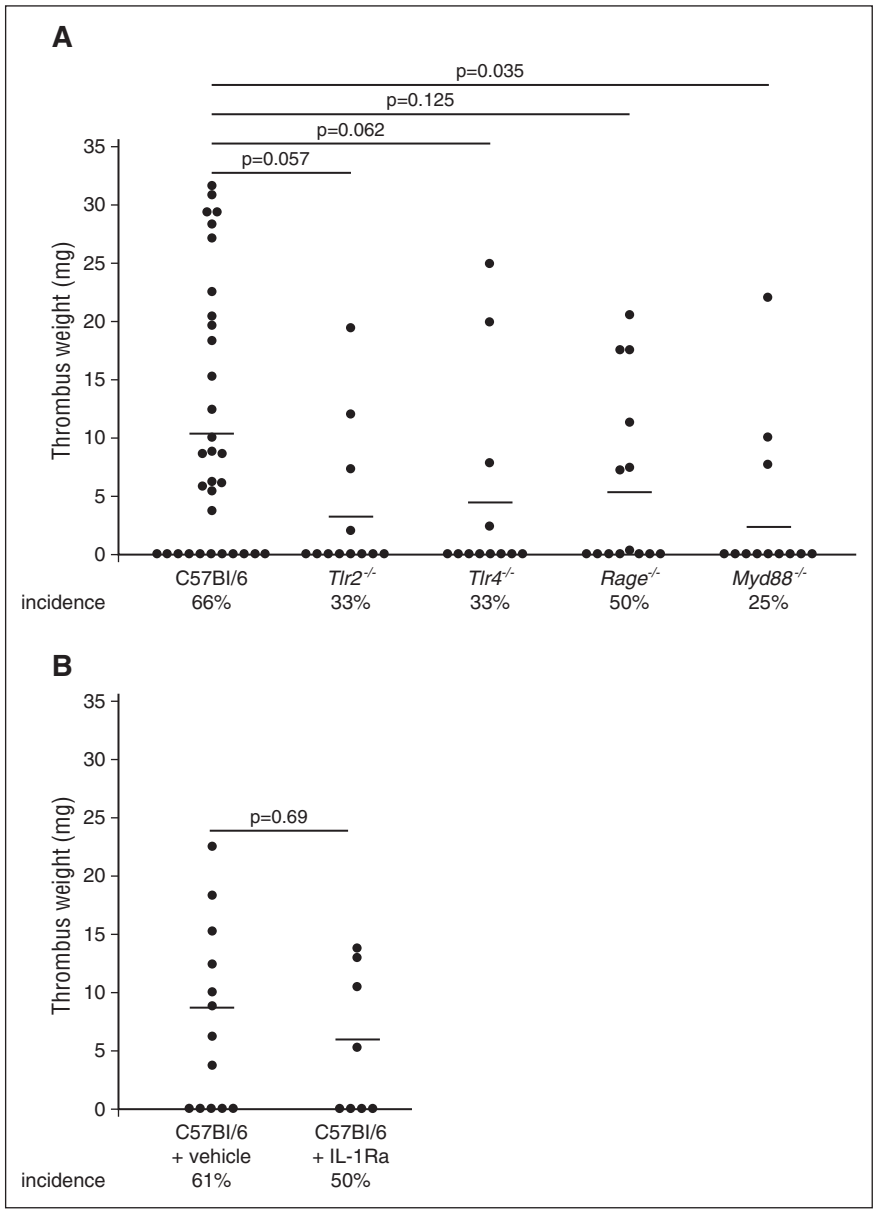

Figure 3. Redundant pattern recognition receptors mediate the prothrombotic effects of HMGB1. (A) Thrombus weight in C57Bl/6 mice (n = 32) compared with *Tlr2*$^{-/-}$ mice (n = 12), *Tlr4*$^{-/-}$ mice (n = 12), *Rage*$^{-/-}$ mice (n = 14), *Myd88*$^{-/-}$ mice (n = 12). Lines indicate mean. One-way ANOVA followed by LSD–post hoc test was used to compare results between groups. (B) Thrombus weight in C57Bl/6 mice receiving vehicle (n = 13) compared with anakinra s.c. (n = 8). Lines indicate mean. The Student *t* test was used to compare results between groups.

NET formation

Blood from healthy human donors was collected in lithium-heparin tubes and centrifuged with Ficoll Paque Plus. Erythrocytes were lysed and neutrophils were plated on poly-L-lysine–coated coverslips and incubated for 1 hour with buffer, disulfide, sulfonyl, or 3S- HMGB1 (1 μg/mL) in the presence of 20 μg/mL aprotinin and fixed with acetone. Samples were blocked with 5% goat serum and stained with a rabbit anti-human MPO antibody (polyclonal; DAKO) followed by a secondary antibody (goat anti-rabbit AlexaFlour 594; Invitrogen). DNA of cell nuclei was stained with Hoechst.

Thromboelastometry

Citrated whole blood from C57BL/6 mice which received 2 mg/kg 3S-, disulfide, or sulfonyl HMGB1 was compared with buffer. For extem measurements, blood was recalcified by adding startem reagent, whereas the coagulation was initiated by extem reagent (Tem Innovations). In Fibtem measurements, platelets were inactivated via cytochalasin D. For analysis, a rotation thromboelastometry device was used (ROTEG 05; Pentapharm).

Statistical analysis

All data are shown as mean ± standard error of the mean (SEM), unless indicated otherwise. Thrombus weight was tested for normal distribution using the Kolmogorov-Smirnov test and the independent samples *t* test was performed to compare groups (SPSS). More than 2 groups were compared using the analysis of variance (ANOVA) followed by least significant difference (LSD)–post hoc test. A value of $P < .05$ was considered significant.

Figure 2 (continued) representative of n = 3 experiments. (D) Immunofluorescence staining of cross-sections of the IVC 48 hours after flow reduction. Top, Presence of HMGB1 on NETs (arrowheads) as shown by staining for HMGB1 (green), Ly6G (red), and DAPI (blue); bar, 20 μm. Bottom, HMGB1 (green) colocalizes with platelets (red). Dotted line indicates endothelium; bar, 100 μm. Nuclei are counterstained with DAPI (blue). Images representative of n = 3 experiments. (E) Thrombus weight in *Hmgb1*$^{+/+}$ fetal liver cell chimeras (n = 7) compared with *Hmgb1*$^{-/-}$ chimeras (n = 6). (F) Thrombus weight in *Hmgb1*$^{-/-}$ bone marrow chimeras (n = 6) compared with *Hmgb1*$^{-/-}$ chimeras receiving wild-type platelets (n = 10), *Hmgb1*$^{-/-}$ platelets (n = 8), or wild-type neutrophils (n = 9). (A,E,F) Line indicates mean. The Student *t* test was used to compare results between 2 groups, 1-way ANOVA followed by LSD–post hoc test for 3 groups.

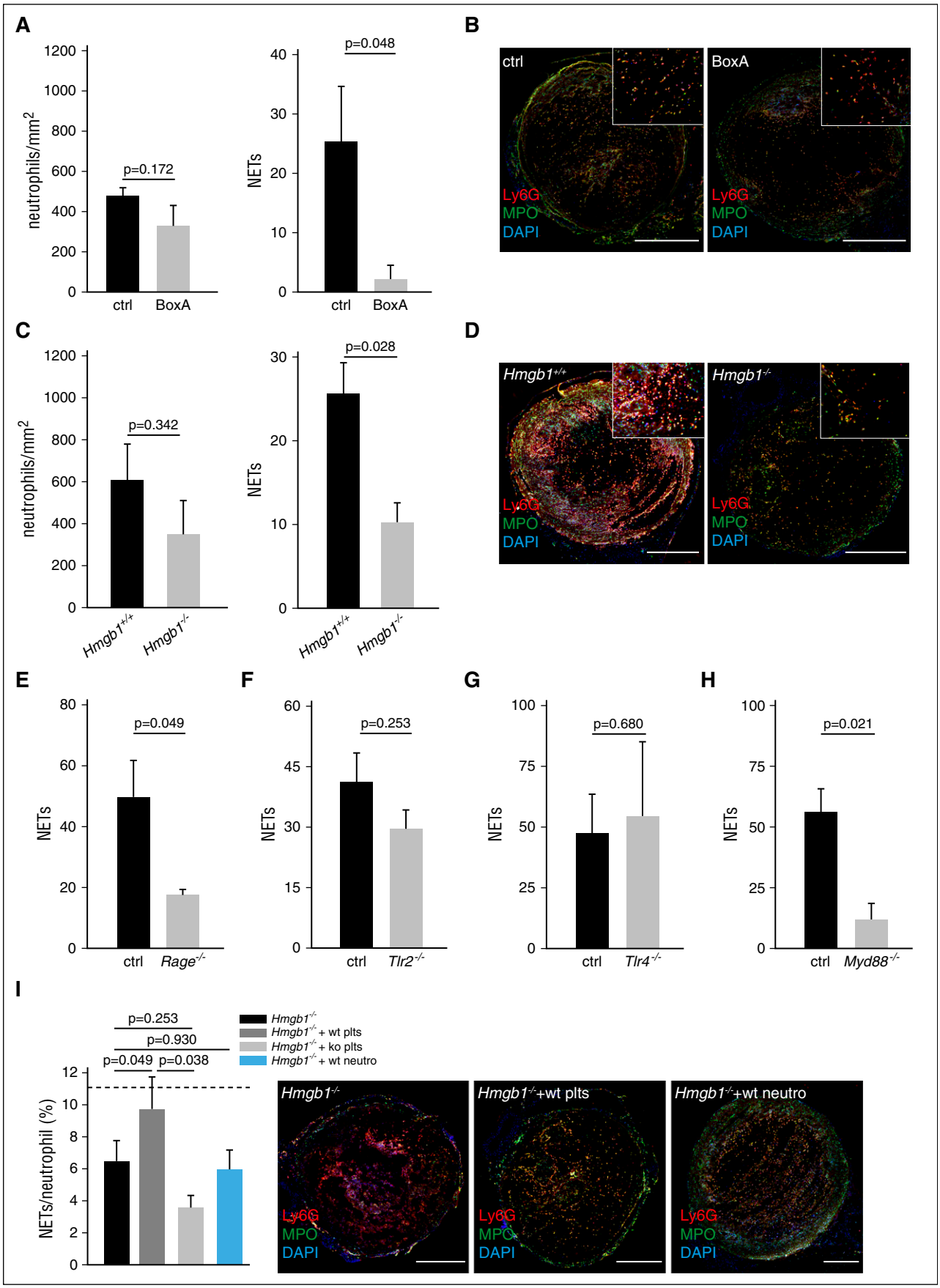

Figure 4.

Results

Progressive accumulation of HMGB1 in the developing venous thrombus

To examine the importance of HMGB1 for venous thrombosis, we used a previously described mouse model of flow reduction in the IVC,[6] which can be monitored noninvasively by Doppler ultrasound (supplemental Figure 1A; supplemental Video 1-2, available on the *Blood* Web site). After 48 hours, a thrombus develops upstream of the stenosis in the IVC as shown by CT in vivo (supplemental Figure 1B; supplemental Video 3). To our surprise, we observed that HMGB1 progressively accumulates at the luminal aspect of the IVC endothelium and can already be detected prior to thrombus formation. As early as 1 hour after induction of flow restriction, small amounts of HMGB1 are observed close to the endothelium (Figure 1A). At 6 hours, the endothelium is decorated by large amounts of HMGB1, which fill the entire IVC lumen at 12 hours. Local HMBG1 deposition is paralleled by the gradual accumulation of leukocyte-platelet aggregates as shown by electron and intravital 2-photon microscopy (Figure 1).

HMGB1 in DVT originates from platelets and neutrophils

Because HMGB1 progressively accumulates inside the IVC following flow restriction, we next assessed whether this mediator of sterile inflammation is of any biological relevance for the thrombotic processes driving DVT formation. To test this, we determined the effect of pharmacological inhibition of HMGB1 on DVT development. Briefly, we treated Balb/c mice prior to flow restriction with the HMGB1 inhibitor BoxA, which has been reported to attenuate sepsis as well as hepatitis B virus–induced hepatitis.[15,18,33] BoxA treatment resulted in significantly decreased thrombus weight and also showed a trend toward a moderately reduced incidence of DVT (Figure 2A). This suggests that HMGB1 propagates and accelerates thrombus formation.

But what is the source of luminal HMGB1 deposition during DVT formation? HMGB1 can get access to the extracellular compartment by release from necrotic cells. However, only very few necrotic cells could be observed within the lumen of the IVC in the initial stages of DVT and endothelial cell necrosis was virtually absent (Figure 2B). Besides its passive leakage from dead cells, HMGB1 can also be actively released by hematopoietic cells, including leukocytes and platelets.[11-13] To dissect the source of HMGB1, we stained for this DAMP in developing venous thrombi. At early stages of DVT, most of HMGB1 was associated with platelets (Figure 2C), which have been reported to expose HMGB1 on their surfaces upon activation.[11,12,34,35] At later stages, we found colocalization of HMGB1 not only with platelets, but also with NETs (Figure 2D).

To address the importance of blood cell-derived HMGB1 for venous thrombogenesis, we next generated bone marrow chimeras from fetal liver cells of *Hmgb1*$^{-/-}$ mice. *Hmgb1*$^{-/-}$ fetal liver cell chimeras showed significantly reduced thrombus weight and also a reduced incidence of DVT formation compared with *Hmgb1*$^{+/+}$ chimeras (Figure 2E). Next, we dissected the exact cellular source of hematopoietic cell-derived HMGB1 that triggers thrombus formation. To evaluate the importance of platelet- or neutrophil-derived HMGB1 on DVT, we infused wild-type platelets or wild-type neutrophils into *Hmgb1*$^{-/-}$ bone marrow chimeras. Wild-type platelets fully restored DVT formation compared with *Hmgb1*$^{-/-}$ platelets, whereas wild-type neutrophils ($P = .096$) had no significant effect (Figure 2F). Correspondingly, no HMGB1 could be detected within the vessel lumen of *Hmgb1*$^{-/-}$ chimeras, but the amount of HMGB1 was increased in chimeras supplemented with wild-type platelets, and to a lesser degree in chimeras supplemented with wild-type neutrophils (supplemental Figure 1C).

Redundant pattern recognition receptors mediate the prothrombotic effects of HMGB1

Having identified blood-borne HMGB1 as a major propagator of DVT, we next addressed the importance of distinct receptors in mediating HMGB1's prothrombotic effects (Figure 3A). First, we focused on TLR2, which is expressed on myeloid leukocytes as well as platelets.[36] Genetic ablation of this receptor decreased the incidence of DVT, but had no significant effect on thrombus weight. Another well-characterized receptor for HMGB1 is TLR4, which is expressed on myeloid leukocytes, platelets, and endothelial cells.[37] Loss of TLR4 had no significant effect on DVT formation. The HMGB1-RAGE axis has been shown to be important for mediating leukocyte accumulation and subsequent tissue damage.[11,38,39] *Rage*$^{-/-}$ mice also showed no significant reduction in DVT formation. Because none of these pattern recognition receptors could significantly decrease thrombus formation, we tested whether combined inhibition, through deficiency of the adaptor molecule Myd88, which is involved in downstream signaling of many TLRs including TLR2, TLR4, as well as RAGE, would result in a more pronounced phenotype.[14,40] Indeed, *Myd88*$^{-/-}$ mice had significantly reduced thrombus weight and a low incidence of DVT (Figure 3A). Because Myd88 is also important for IL-1 receptor signaling, we analyzed the contribution of this pathway to venous thrombosis by using an IL-1 receptor antagonist in C57Bl/6 mice, but this treatment had no influence on DVT (Figure 3B).[41] Taken together, the above data show that TLR2, TLR4, and RAGE play redundant functions during DVT and only combined deficiency in converging signaling pathways of these receptors inhibits thrombus formation.

HMGB1 influences neutrophil recruitment and NET formation

Because blood-derived HMGB1 facilitates and propagates venous thrombosis, we next focused on the underlying cellular and molecular mechanisms. Previously, we and others have shown that in venous thrombosis, clot formation depends on leukocyte recruitment.[6,42,43]

Figure 4. HMGB1 induces NET formation trough RAGE in DVT. (A-I) Quantification of neutrophils and NETs. Results are mean ± SEM. (A) BoxA (n = 5) compared with control (n = 5). (B) Immunofluorescence staining for Ly6G (red) and MPO (green) from cross-sections of the IVC 48 hours after flow reduction of BoxA-treated (bottom) or control mice (top). Nuclei are counterstained with DAPI (blue); bar, 200 μm. (C) *Hmgb1*$^{-/-}$ (n = 3) fetal liver cell chimeras compared with *Hmgb1*$^{+/+}$ chimeras (n = 5). (D) Immunofluorescence staining for Ly6G (red) and MPO (green) from cross-sections of the IVC 48 hours after flow reduction of *Hmgb1*$^{+/+}$ (top) or *Hmgb1*$^{-/-}$ fetal liver cell chimeras (bottom). Nuclei are counterstained with DAPI (blue); bar, 200 μm. (E) Quantification of NETs in *Rage*$^{-/-}$ mice compared with control (n = 5 each). (F) Quantification of NETs in *Tlr2*$^{-/-}$ mice compared with control (n = 3 each). (G) Quantification of NETs in *Tlr4*$^{-/-}$ mice compared with control (n = 3 each). (H) Quantification of NETs in *Myd88*$^{-/-}$ mice compared with control (n = 3 each). (I) Left, NET formation capacity shown as NETs/neutrophil (n = 5 each) in *Hmgb1*$^{-/-}$ chimeras compared with *Hmgb1*$^{-/-}$ chimeras receiving wild-type platelets or wild-type neutrophils. Dotted line indicates mean in *Hmgb1*$^{+/+}$ bone marrow chimeras. Right, Immunofluorescence staining for Ly6G (red) and MPO (green) from cross-sections of the IVC 48 hours after flow reduction in *Hmgb1*$^{-/-}$ chimeras compared with *Hmgb1*$^{-/-}$ chimeras receiving wild-type platelets, *Hmgb1*$^{-/-}$ platelets or wild-type neutrophils. (n = 3 each). Nuclei are counterstained with DAPI (blue); bar, 200 μm. The Student *t* test was used to compare results between 2 groups, 1-way ANOVA followed by LSD–post hoc test for 3 groups.

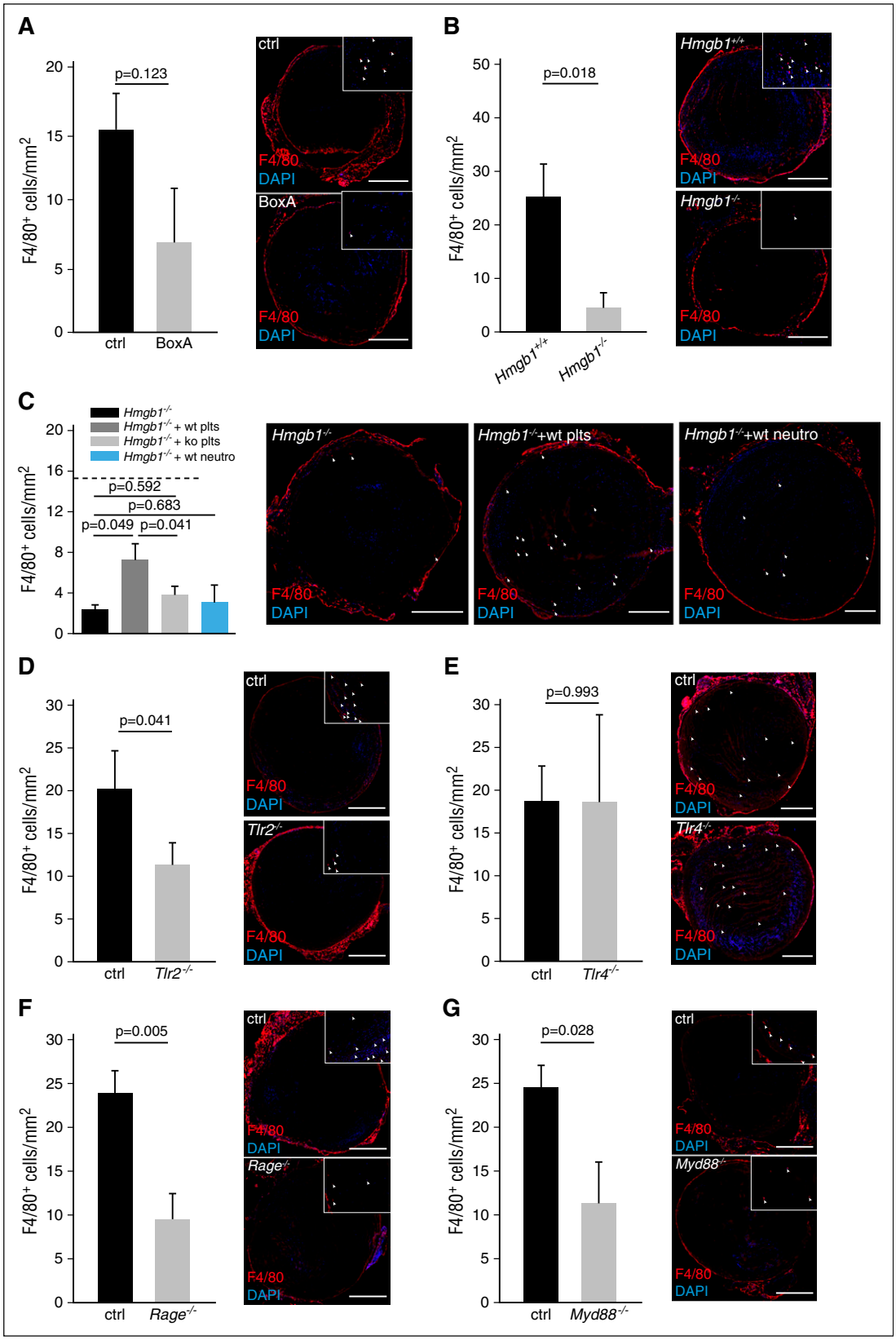

Figure 5. Platelet derived HMGB1 promotes monocyte recruitment. (A-G) Left, Quantification of monocytes. Results are mean ± SEM. Right, Immunofluorescence staining for F4/80 (red) from cross-sections of the IVC. Nuclei are counterstained with DAPI (blue); arrowheads indicate individual monocytes at higher magnification; bar, 200 μm. Images representative of n = 3 experiments. (A) BoxA compared with control (n = 5 each). (B) *Hmgb1*$^{-/-}$ (n = 3) fetal liver cell chimeras compared with *Hmgb1*$^{+/+}$ chimeras (n = 5). (C) *Hmgb1*$^{-/-}$ chimeras compared with *Hmgb1*$^{-/-}$ chimeras receiving wild-type platelets, *Hmgb1*$^{-/-}$ platelets, or wild-type neutrophils. Dotted line indicates mean in *Hmgb1*$^{+/+}$ bone marrow chimeras (n = 3 each). (D) *Tlr2*$^{-/-}$ compared with control (n = 4 each). (E) *Tlr4*$^{-/-}$ compared with control (n = 4 each). (F) *Rage*$^{-/-}$ compared with control (n = 5 each). (G) *Myd88*$^{-/-}$ compared with control (n = 4 each). The Student *t* test was used to compare results between 2 groups, 1-way ANOVA followed by LSD–post hoc test for 3 groups.

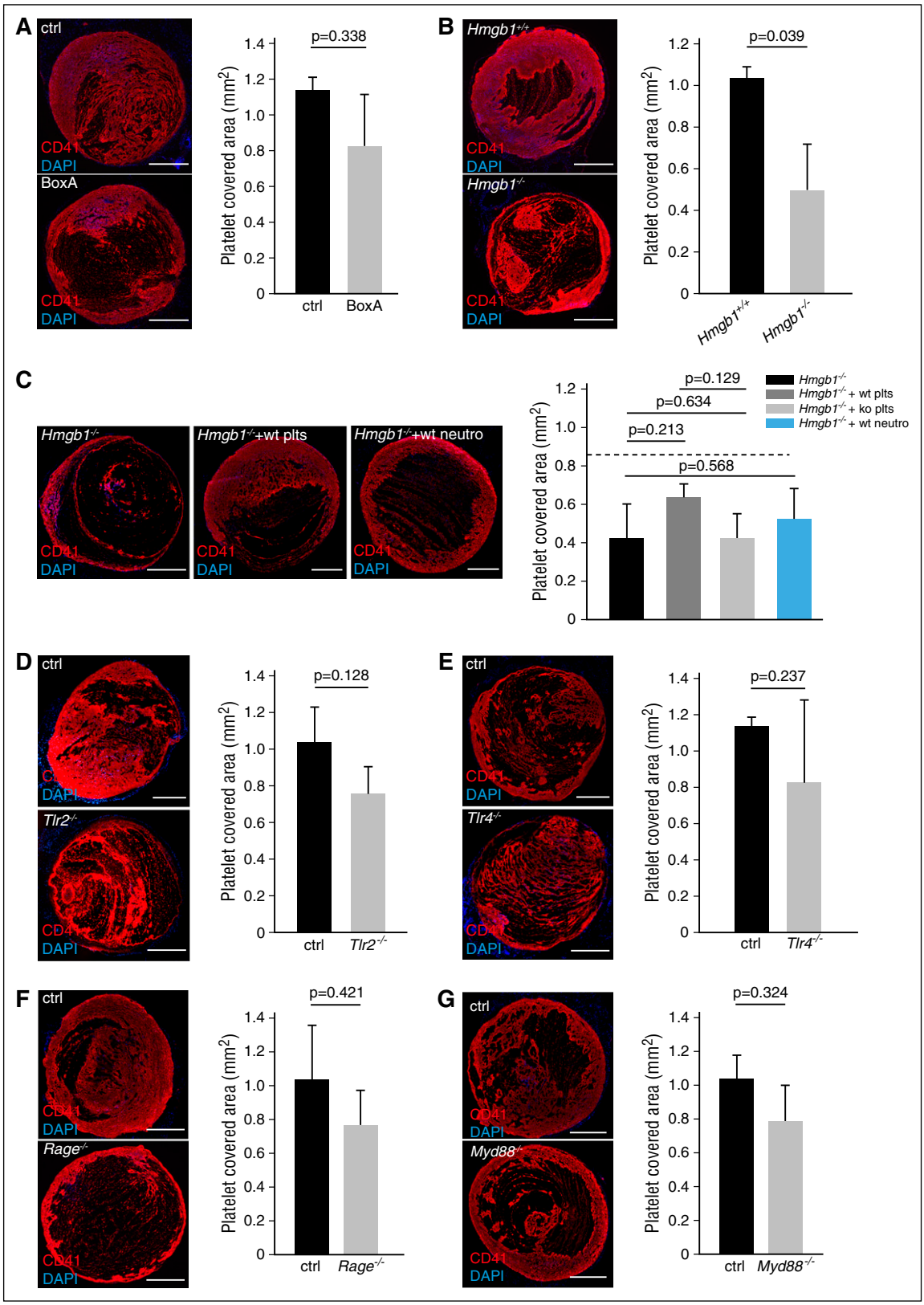

Figure 6. HMGB1 contributes to platelet accumulation in venous thrombosis. (A-G) Left, Immunofluorescence staining for CD41 (red) from cross-sections of the IVC. Nuclei are counterstained with DAPI (blue); bar, 200 μm. Images representative of n = 3 experiments. Right, Quantification of platelet-covered area. Results are mean ± SEMT. (A) BoxA compared with control (n = 5 each). (B) *Hmgb1*$^{-/-}$ fetal liver cell chimeras (n = 3) compared with *Hmgb1*$^{+/+}$ chimeras (n = 5). (C) Left, Immunofluorescence for CD41 in *Hmgb1*$^{-/-}$ chimeras compared with *Hmgb1*$^{-/-}$ chimeras receiving wild-type platelets, *Hmgb1*$^{-/-}$ platelets, or wild-type neutrophils (n = 3 each). Right, Quantification of platelet-covered area. Dotted line indicates mean in *Hmgb1*$^{+/+}$ bone marrow chimeras (n = 3 each). (D) *Tlr2*$^{-/-}$ compared with control (n = 3 each). (E) *Tlr4*$^{-/-}$ compared with control (n = 3 each). (F) *Rage*$^{-/-}$ compared with control (n = 5 each). (G) *Myd88*$^{-/-}$ compared with control (n = 3 each). The Student *t* test was used to compare results between 2 groups, 1-way ANOVA followed by LSD–post hoc test for 3 groups.

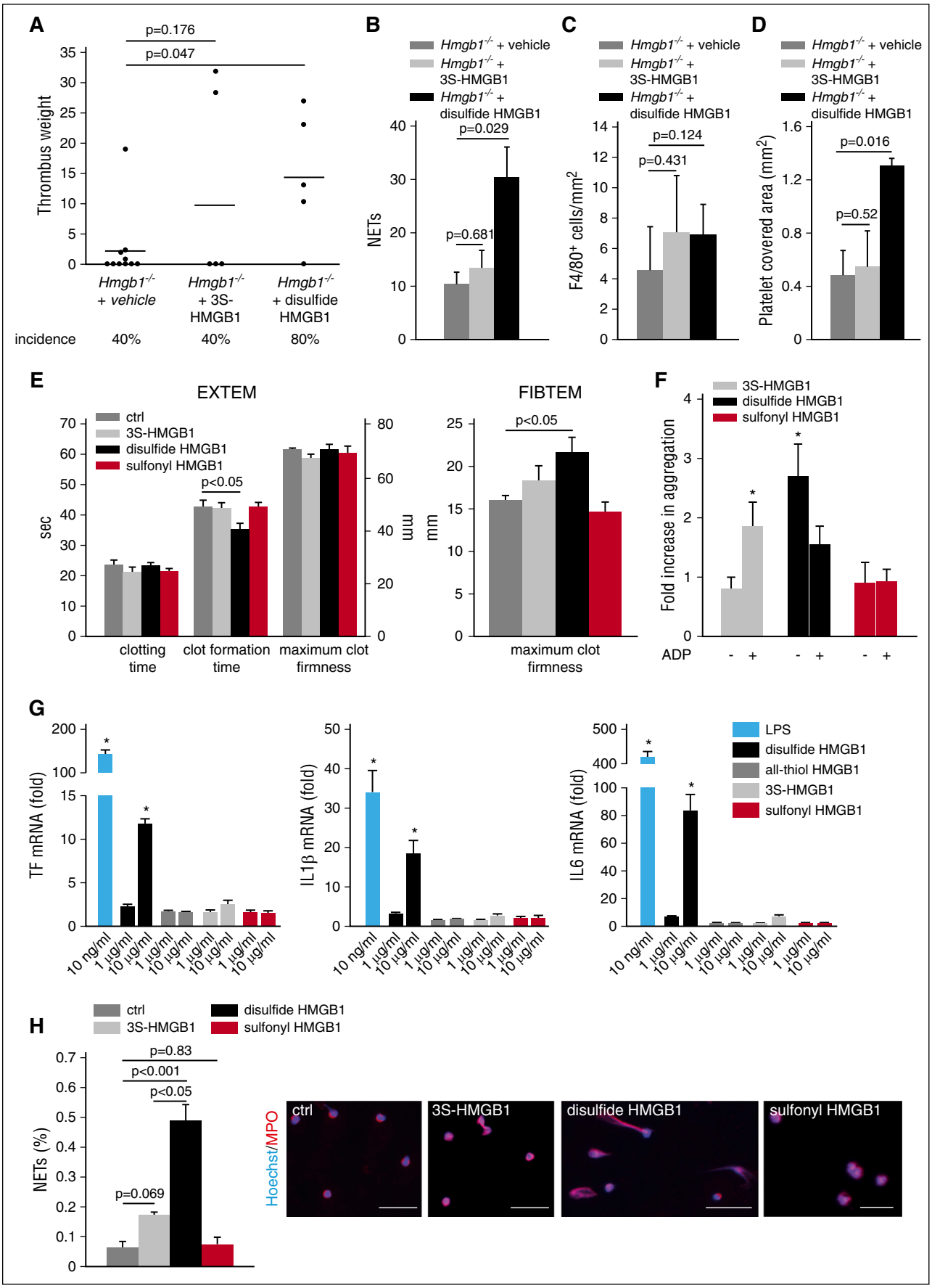

Figure 7.

Therefore, we determined the effect of HMGB1 inhibition by BoxA on initial leukocyte accumulation by intravital microscopy and found a significant reduction in BoxA-treated animals (supplemental Figure 1D). Because neutrophils play an important role in DVT formation,[2,5,6] propagating the thrombotic process by releasing prothrombotic NETs,[6,44-47] we next focused on this leukocyte subset. Inhibition of HMGB1 or lack of blood cell-derived HMGB1 had no significant effect on neutrophil accumulation, but significantly reduced NET formation (Figure 4A-D), suggesting that HMGB1 acts prothrombotic at least in part by supporting NETosis. Specificity of the staining was confirmed through isotype control antibodies (supplemental Figure 2A). Consistent with the finding that HMGB1 boosts NET formation through RAGE in vitro,[11] NETosis during DVT formation was virtually abolished in mice lacking RAGE, whereas TLR2 and TLR4 appear to be dispensable for this process. Also, *Myd88*$^{-/-}$ mice had a significantly decreased NET formation (Figure 4E-H; supplemental Figure 2B-E). Infusion of WT platelets, but not of *Hmgb1*$^{-/-}$ platelets or WT neutrophils, into HMGB1-null chimeras rescued the capacity of HMGB1-null neutrophils to form NETs (Figure 4I; supplemental Figure 2F). Together, these data implicate that platelet-derived HMGB1 increases the capacity of neutrophils to form NETs in a process largely mediated by RAGE in vivo.

Platelet derived HMGB1 supports monocytes accumulation

Although neutrophils are mainly important for propagation of DVT by activating the intrinsic pathway of coagulation, monocytes initiate clot formation by delivering TF that activates the extrinsic pathway.[4,6] Inhibition of HMGB1 through BoxA resulted in a significantly decreased monocyte recruitment as visualized by intravital microscopy (supplemental Figure 3A). Deficiency of blood cell-derived HMGB1 resulted in significantly reduced monocyte accumulation within the thrombus after 48 hours, which could be significantly increased by WT platelets, but not by *Hmgb1*$^{-/-}$ platelets nor by wild-type neutrophils (Figure 5A-C; supplemental Figure 3B). The DAMP receptors RAGE and TLR2 mediated HMGB1-dependent monocyte accumulation through Myd88, whereas TLR4 had no significant effect (Figure 5D-G). In summary, platelet-derived HMGB1 supports monocyte recruitment to the developing venous thrombus through RAGE and TLR2 in a Myd88-dependent manner.

HMGB1 fosters platelet accumulation in venous thrombosis

Having shown that platelet HMGB1 drives sterile inflammation during DVT, we next asked whether it also impacts on platelet recruitment during venous thrombogenesis. Indeed, platelets do not only release HMGB1, but are also activated by the DAMP in an autocrine/paracrine manner.[11,12,17,48,49] We found that BoxA treatment and even more so lack of blood cell-derived HMGB1 decreased platelet recruitment particularly at early stages of thrombus formation as assessed by intravital microscopy and histology (Figure 6A-B; supplemental Figure 3C-D). Reconstitution of *Hmgb1*$^{-/-}$ bone marrow chimeras with wild-type platelets resulted in a trend toward increased platelet accumulation, whereas wild-type neutrophils had no effect (Figure 6C). TLR2, TLR4, RAGE, and Myd88 deficiency each had no significant effect on platelet accumulation after 48 hours (Figure 6D-G). Hence, platelets are not only a source of HMGB1 in DVT, but their early recruitment at the site of thrombus formation is also promoted by HMGB1.

HMGB1 is rendered prothrombotic by oxidation

Because HMGB1 not only boosts innate immune cell accumulation but also modulates the activation of inflammatory cells depending on the redox state, we next determined whether the prothrombotic effect of HMGB1 is influenced by oxidation.[15] Infusion of nonoxidizable 3S-HMGB1 into *Hmgb1*$^{-/-}$ chimeras could not significantly increase thrombus formation and had no impact on the incidence of thrombosis. However, disulfide HMGB1 significantly increased thrombus weight as well as the incidence of thrombosis (Figure 7A). Analysis of these thrombi indicated that disulfide HMGB1 significantly increased NET formation and platelet accumulation compared with *Hmgb1*$^{-/-}$ chimeras, whereas monocyte recruitment could be only increased nonsignificantly by both HMGB1 redox forms (Figure 7B-D; supplemental Figure 3E-F).

Next, we determined in vitro whether the prothrombotic effect of HMGB1 depends on the redox state. First, we determined the redox form of HMGB1 in resting as well as activated platelets by mass spectrometry: resting platelets contained reduced HMGB1, whereas stimulation of platelet-rich plasma with thrombin resulted in the formation of sulfonyl HMGB1 within 30 minutes (supplemental Figure 4A-B). However, only disulfide HMGB1 significantly decreased clot formation time in extem tests indicating an effect on platelets, whereas neither nonoxidizable 3S-HMGB1 nor sulfonyl HMGB1 had an effect (Figure 7E). To analyze the impact of the HMGB1 redox forms on platelets in more detail, we performed whole-blood aggregometry, where also only disulfide HMGB1 significantly increased aggregation. In addition, we assessed whether the different redox forms might sensitize platelets for a following stimulus and preincubated whole blood first with HMGB1 and then stimulated it with ADP. In this setting, only the nonoxidizable form had a significant effect. The aggregation induced by disulfide HMGB1 could not be augmented further by subsequent stimulation with ADP (Figure 7F). Because, disulfide HMGB1 significantly increased maximum clot firmness in the Fibtem assay, excluding an effect on platelets, we investigated the effect of HMGB1 on TF expression in monocytes, which are the main source of TF in DVT (Figure 7E).[6] Using real-time reverse transcriptase polymerase chain reaction (RT-PCR), we could show that only disulfide HMGB1 induced a significant upregulation of TF as well as of the cytokines IL-6 and IL-1β (Figure 7G). Finally, we characterized the impact of the HMGB1 redox forms on NET formation in vitro: disulfide HMGB1 was significantly more potent in inducing NETosis than the reduced form, consistent with the in vivo results (Figure 7H). These differences in the biological effect of different

Figure 7. The prothrombotic effects of HMGB1 depend on the redox state. (A) Thrombus weight in *Hmgb1*$^{-/-}$ chimeras (n = 10) treated with buffer compared with *Hmgb1*$^{-/-}$ chimeras (n = 5 each) receiving 3S- or disulfide HMGB1. Lines indicate mean. (B) Quantification of NETs, (C), monocytes, (D), and platelet covered area from immunofluorescence stainings of *Hmgb1*$^{-/-}$ chimeras receiving buffer, 3S-, or disulfide HMGB1 (n = 3 each). (E) Extem (left) and Fibtem (right) 6 hours after IV injection of 3S- (n = 3), disulfide HMGB1 (n = 3), or sulfonyl (n = 3) compared with control (n = 5). (F) Fold increase in whole-blood aggregation after incubation with 3S-, disulfide, or sulfonyl HMGB1 compared with control stimulated with buffer. This was followed by stimulation by ADP in the groups indicated (n = 4-6). (G) Results from RT-PCR for TF (left), IL-1β (middle), and IL-6 (right) of peripheral blood human monocytes incubated with different redox forms of HMGB1 and LPS for 3 hours shown as fold increase compared with control stimulated with the respective buffer (n = 3 each). (H) Left, Quantification of NET formation in vitro after stimulation of isolated human neutrophils with buffer, 3S-, disulfide, or sulfonyl HMGB1 (n = 3 each). Right, Representative images of immunofluorescence stainings for MPO (red) and Hoechst (blue); bar, 50 μm. Results are mean ± SEM. *$P < .05$. The Student *t* test was used to compare results between 2 groups, 1-way ANOVA followed by LSD–post hoc test for 3 groups.

HMGB1 redox forms could be explained by their differential binding to RAGE: SPR analysis showed a higher association rate of disulfide HMBG1 to RAGE compared with nonoxidizable HMBG1 and sulfonyl HMBG1 at first glance. Because the sensorgrams did not follow a typical 1:1 binding shape, we performed IM analysis to discriminate between the different binding events. Interestingly, IM analysis revealed 2 high-affinity binding events of nonoxidizable HMBG1 (6 nM and 32 nM) and sulfonyl HMBG1 (0.2 nM and 120 nM) to RAGE. Whereas the overall affinities of the lower-affinity binding events are similar for all 3 RAGE redox forms, the higher-affinity binding event is indeed shaped not only by a higher association rate for disulfide HMGB1, but also to a drastically higher dissociation rate. For the sulfonyl HMGB1, the high-affinity binding is barely detectable (12% peak weight) and might explain its biological inactivity (supplemental Figure 4 C-E). In conclusion, reduced HMGB1 released from platelets is rendered prothrombotic by oxidation and disulfide HMGB1 induces platelet aggregation, NET formation, and TF production in monocytes.

Discussion

DVT is one of the most common cardiovascular disorders and has to be considered a sterile inflammatory process that results in vessel occlusion due to aberrant activation of immunothrombosis.[3] Targeting the inflammatory response that culminates in DVT formation could therefore represent a promising strategy to treat or prevent DVT formation without affecting physiological hemostasis. However, although the cells triggering DVT formation have largely been identified over the past years, the molecular cascades involved in translating sterile inflammation into a thrombotic disorder remain incompletely understood.[2,4-6,45]

Here, we identified HMGB1 as the key factor in the reciprocal communication between platelets, neutrophils, and monocytes inducing clot formation.[6] We demonstrate that platelets deliver reduced HMGB1 to the affected vein thereby inducing the recruitment and activation of innate immune cells, particularly monocytes, in a process involving RAGE, TLR2, and Myd88. Platelet-derived disulfide HMGB1 also boosts monocyte TF and cytokine expression, triggers the formation of prothrombotic NETs, and supports platelet accumulation in an autocrine/paracrine fashion. Enhanced platelet accumulation and NETosis in turn results in additional HMGB1 deposition setting off a vicious circle propagating DVT formation (supplemental Figure 5). Notably, unlike loss of blood cell-derived HMGB1, deficiency of the known HMGB1 receptors TLR2, TLR4, or RAGE was not sufficient to inhibit venous thrombus formation, but combined deficiency of downstream signaling in *Myd88*$^{-/-}$ mice significantly reduced thrombus formation. A contribution of the IL-1 receptor, which also signals through Myd88, on thrombus formation could be excluded. This indicates that HMGB1 acts on all receptors synergistically and that these receptors have redundant functions in DVT formation. Hence, our study identifies HGMB1 as a potential new target for the treatment and prevention of DVT.

HMGB1 is a ubiquitous protein primarily found in the cell nucleus and upon activation of cells HMGB1 can be actively secreted into the extracellular space. In addition, cell necrosis results in uncontrolled release of HMGB1 into the extracellular compartment.[16,39] The pathophysiological importance of HMGB1 as a trigger of inflammatory responses has been documented in several disease settings, particularly sepsis, where disseminated intravascular coagulation is augmented by HMGB1[50] and even late inhibition of HMGB1 resulted in improved survival in mice.[10] In the setting of experimental microvascular thrombosis induced by $FeCl_3$, platelet-derived HMGB1 has recently been demonstrated to contribute to the inflammatory response and small vessel occlusion.[17] Moreover, HMGB1 contributes to ischemia/reperfusion injury and has been shown to be a critical mediator of sterile muscle injury as seen in trauma.[15,51-53]

We could show here that during DVT, HMGB1 accumulates in the absence of overt luminal or vascular cell necrosis and is delivered by blood cells, mainly platelets, but at later stages also by NETting neutrophils. In line with that, HMGB1 could be detected during the resolution phase of DVT in murine venous thrombi.[54] It has been shown previously that platelets actively expose HMGB1 on their surfaces after activation in vitro.[12,48] In line with our observation in mice, HMGB1 has recently been reported in human coronary artery thrombi, where it also colocalized with platelets and NETs.[11,34,35] This is in contrast to scenarios dominated by tissue necrosis, where HMGB1 mostly derived from dying cells within the tissue is important for induction of the inflammatory response.[55] Therefore, we could identify activated platelets as the main source of HMGB1 in venous thrombosis in vivo.

But how is HMGB1 involved in the prothrombotic cross-communication between platelets, monocytes, and neutrophils promoting venous thrombosis formation? For recruitment of innate immune cells, mainly reduced all-thiol HMGB1 is important, which is present in resting platelets and exposed after activation.[35,56] Once recruited to the vessel wall, myeloid leukocytes and activated platelets in turn release reactive oxygen species, resulting in the formation of disulfide HMGB1.[15,35] It has been shown recently that in the extracellular space HMGB1 is oxidized quickly: the half-life for all-thiol HMGB1 within the serum is 17 minutes before it is oxidized into disulfide HMGB1 in vitro.[57] In addition, in a model of ischemic stroke mainly all-thiol HMGB1 is found after 2 hours in serum samples, whereas both all-thiol and disulfide HMGB1 are found after 24 hours.[32] Therefore, reduced HMGB1 released from platelets is probably oxidized quickly within the blood stream. Disulfide HMGB1 activates immune cells and, as we show here, has profound prothrombotic effects by promoting formation of NETs, platelet aggregation, and TF expression of monocytes. Terminal oxidation to the inert sulfonyl form of HMGB1 prevents an overshooting immune response. This could be explained by different binding characteristics of the HMGB1 redox forms to RAGE. SPR and IM analysis suggest 2 binding sites for HMBG1 on RAGE. In line with this, a second binding epitope of HMGB1 to RAGE has been proposed recently.[58] So far, only 1 binding site for HMGB1 on RAGE has been identified, but this was never analyzed with different HMGB1 redox forms.[59-61] Whereas 1 of the 2 potential binding sites can be bound similarly by the different HMBG1 redox variants, the other site probably discriminates between the different redox states. We report here that RAGE, but not TLR2/4, is involved in NETosis induced by platelet-derived HMGB1 in venous thrombosis. NETs in turn, provide a prothrombotic scaffold and expose even more disulfide HMGB1 on their extracellular DNA strands.[62] Moreover, NETs have been shown to contribute to venous as well as arterial thrombosis through other mechanisms,[6,44,46,47] including their ability to bind and/or activate platelets, TF, and FXII altogether leading to acceleration of thrombus formation.[36,45,63]

In addition to neutrophils, monocytes are essential for venous thrombosis because they are the main source of blood-derived TF in this model.[4,6] It has been demonstrated that HMGB1 induces monocyte migration in vitro mediated by forming a complex with CXCL12 and activating the CXCR4 receptor, while RAGE also contributes.[64] Interestingly, heparin inhibits the binding of HMGB1 to macrophages, thereby preventing their activation, a mechanism that might contribute

to heparin's antithrombotic activity.[65] Here, we show in vivo that platelet-derived HMGB1 is essential for the recruitment and accumulation of monocytes in the setting of venous thrombosis through RAGE and TLR2. Moreover, we could show that disulfide HMGB1 induces the expression of TF, IL-6, and IL-1β in monocytes. This initiates the extrinsic pathway of coagulation and augments the activation status of innate immune cell. Treatment of mice with the competitive HMGB1 antagonist BoxA significantly decreased thrombus weight, but had no effect on the incidence of thrombosis, implicating that BoxA impairs propagation of thrombosis rather than its initiation and is less potent than deficiency of blood-derived HMGB1. Consistent with this, initial monocyte recruitment was impaired, but accumulation of monocytes was not significantly reduced in BoxA-treated mice, whereas NET formation was abolished, which is mainly implicated in propagation of venous thrombosis. Because HMGB1 induces the expression of several chemokines and cytokines in addition to its promigratory effects, long-term inhibition of HMGB1 could potentially impair immune responses.[15,16,37,55,64,66,67] However, inhibition of HMGB1 over several days to weeks in the setting of arthritis and atherosclerosis in mice had no reported negative effect and mice were not prone to infection.[68,69] In addition, inhibition of HMGB1 in sepsis reduced lethality indicating that it could be a target for regulation of overshooting immune responses.[10,18] However, the long-term effects of HMGB1 inhibition in humans might be different to mice.

During DVT, HMGB1 does not only coordinate sterile inflammation, but also directly acts on platelets in an autocrine/paracrine manner supporting platelet recruitment in a positive feedback loop. This in turn facilitates further leukocyte recruitment, monocyte activation, and boosts NET formation.[6] But how exactly does HMGB1 activate platelets? In vitro, it has been shown that HMGB1 can bind to activated platelets via RAGE and TLR4, leading to platelet activation in the latter setting.[34,49] For microvascular thrombosis, signaling of HMGB1 through TLR4 and Myd88 has been demonstrated to be involved in platelet activation and granule secretion in vivo.[17] However, this is not exclusive because other DAMPs, including histones, can activate platelets through similar pattern recognition receptor–dependent pathways.[36] In the setting of venous thrombosis, we could not identify a single receptor exclusively mediating all effects of HMGB1 on platelets. This can be explained by the absence of an oxidizing agent like $FeCl_3$ in our model of macrovascular thrombosis in contrast to the previous study addressing microvascular thrombosis.[17] Consistent with this, we show here that the prothrombotic effects of HMGB1 depend on the redox state of the DAMP protein: all-thiol HMGB1 sensitizes platelets toward additional agonists, such as ADP, but has little direct effects on platelet aggregation. In contrast, disulfide HMGB1 causes aggregation of whole blood even in the absence of additional platelet agonists.

In conclusion, using an in vivo model of macrovascular venous thrombosis, we demonstrate that platelets contain all-thiol HMGB1, and are the major source of HMGB1 in DVT. HMGB1 is exposed on the platelet surface in its reduced form, but following release it is rapidly oxidized to the disulfide and sulfonyl forms. The disulfide form of HMGB1 appears to be most relevant for DVT, and in fact we found that 3S-HMGB1, which cannot be oxidized, and the sulfonyl form have a limited impact on DVT. The different forms of redox HMGB1 act via multiple receptors: CXCR4, activated by a complex between reduced HMGB1 and CXCL12; TLR4, activated by disulfide HMGB1; TLR2; and RAGE. Which redox forms interact with TLR2 and RAGE was not previously clear; we provide evidence here that all redox forms of HMGB1 interact with RAGE, except the disulfide form with higher affinity. In venous thrombosis, the order of events starts with luminal accumulation of HMGB, which then (1) recruits and activates monocytes to the developing thrombus, promoting the oxidation to disulfide HMGB1, which in turn provide TF thereby activating the extrinsic pathway of coagulation, and proinflammatory mediators like IL-6 and IL-1β thereby initiating a vicious circle of leukocyte recruitment and activation; (2) induces NET formation through RAGE, which propagates DVT development; (3) synergizes with NET-derived HMGB1 in venous thrombus formation; and finally (4) fosters platelet activation in an autocrine/paracrine manner mediated by oxidized HMGB1. Therefore, different redox forms of HMGB1 orchestrate the interplay between platelets, neutrophils, and monocytes, which is necessary for the development of venous thrombosis in vivo. This DAMP might therefore be an attractive new target for anti-inflammatory strategies in DVT prophylaxis.

Acknowledgments

SPR analyses were performed in the Bioanalytics Core Facility of the Ludwig-Maximilians-Universität (LMU) Biocenter, Munich.

This work was supported by the Deutsche Forschungsgemeinschaft (DFG) through the collaborative research center 914 project B02 (K.S. and S.M.), the Agence Nationale de la Recherche–DFG project JAKPOT (K.S.), Exc 114/2 (K.J.), LMUexcellent (K.S.), the collaborative research center 1123 project A07 (K.S. and S.M.), the German Federal Ministry of Education and Research (BMBF 01EO1503) (C.R.), Associazione Italiana Ricerca sul Cancro (M.E.B.), and the Deutsche Zentrum für Herz-Kreislauf-Forschung (K.S., S.S., C.R., S.J., and S.M.).

Authorship

Contribution: K.S., M.E.B., and S.M. conceived and designed the experiments; V.P., I.S., K.S., M.-L.v.B., and R.C. performed intravital epifluorescence and 2-photon microscopy and, in cooperation with I.L. and M. Schwaiger, performed CT; S.S., K.S., and S.C. planned and performed histological and immunohistochemical analysis; S.R. and I.S. performed ultrasound in mice; A.W. performed electron microscopy; P.H. performed the NET formation assay; J.B. and V.P. performed thromboelastometry; R.H. and K.J. performed and analyzed SPR spectroscopy; D.J.A. performed and analyzed mass spectrometry; A. Antonelli performed real-time RT-PCR and A. Agresti maintained *Hmgb1*$^{-/-}$ mice; M.M., M.L., and F.G. performed aggregometry; V.P., J.B., and I.S. did the surgery for flow reduction in mice; P.P.N. and M. Sperandio provided the *Rage*$^{-/-}$ mice; C.R. and S.J. contributed essential mice; K.S. and S.M. analyzed the data and composed the manuscript; and all authors reviewed the manuscript.

Conflict-of-interest disclosure: M.E.B. is founder and part owner of HMGBiotech, a company that provides goods and services related to HMGB proteins. The remaining authors declare no competing financial interests.

Correspondence: Konstantin Stark, Medizinische Klinik I, Klinikum der Universität München, Marchioninistr 15, 81377 Munich, Germany; e-mail: konstantin.stark@med.uni-muenchen.de.

References

1. Heit JA. Epidemiology of venous thromboembolism. *Nat Rev Cardiol.* 2015;12(8):464-474.
2. Brill A, Fuchs TA, Savchenko AS, et al. Neutrophil extracellular traps promote deep vein thrombosis in mice. *J Thromb Haemost.* 2012;10(1):136-144.
3. Engelmann B, Massberg S. Thrombosis as an intravascular effector of innate immunity. *Nat Rev Immunol.* 2013;13(1):34-45.
4. Mackman N. New insights into the mechanisms of venous thrombosis. *J Clin Invest.* 2012;122(7):2331-2336.
5. Martinod K, Wagner DD. Thrombosis: tangled up in NETs. *Blood.* 2014;123(18):2768-2776.
6. von Brühl ML, Stark K, Steinhart A, et al. Monocytes, neutrophils, and platelets cooperate to initiate and propagate venous thrombosis in mice in vivo. *J Exp Med.* 2012;209(4):819-835.
7. Schulz C, Engelmann B, Massberg S. Crossroads of coagulation and innate immunity: the case of deep vein thrombosis. *J Thromb Haemost.* 2013;11(suppl 1):233-241.
8. Wakefield TW, Myers DD, Henke PK. Mechanisms of venous thrombosis and resolution. *Arterioscler Thromb Vasc Biol.* 2008;28(3):387-391.
9. Chen GY, Nuñez G. Sterile inflammation: sensing and reacting to damage. *Nat Rev Immunol.* 2010;10(12):826-837.
10. Wang H, Bloom O, Zhang M, et al. HMG-1 as a late mediator of endotoxin lethality in mice. *Science.* 1999;285(5425):248-251.
11. Maugeri N, Campana L, Gavina M, et al. Activated platelets present high mobility group box 1 to neutrophils, inducing autophagy and promoting the extrusion of neutrophil extracellular traps. *J Thromb Haemost.* 2014;12(12):2074-2088.
12. Maugeri N, Franchini S, Campana L, et al. Circulating platelets as a source of the damage-associated molecular pattern HMGB1 in patients with systemic sclerosis. *Autoimmunity.* 2012;45(8):584-587.
13. Tang D, Kang R, Zeh HJ III, Lotze MT. High-mobility group box 1, oxidative stress, and disease. *Antioxid Redox Signal.* 2011;14(7):1315-1335.
14. Lotze MT, Tracey KJ. High-mobility group box 1 protein (HMGB1): nuclear weapon in the immune arsenal. *Nat Rev Immunol.* 2005;5(4):331-342.
15. Venereau E, Casalgrandi M, Schiraldi M, et al. Mutually exclusive redox forms of HMGB1 promote cell recruitment or proinflammatory cytokine release. *J Exp Med.* 2012;209(9):1519-1528.
16. Venereau E, Schiraldi M, Uguccioni M, Bianchi ME. HMGB1 and leukocyte migration during trauma and sterile inflammation. *Mol Immunol.* 2013;55(1):76-82.
17. Vogel S, Bodenstein R, Chen Q, et al. Platelet-derived HMGB1 is a critical mediator of thrombosis. *J Clin Invest.* 2015;125(12):4638-4654.
18. Yang H, Ochani M, Li J, et al. Reversing established sepsis with antagonists of endogenous high-mobility group box 1. *Proc Natl Acad Sci USA.* 2004;101(1):296-301.
19. Diaz JA, Obi AT, Myers DD Jr, et al. Critical review of mouse models of venous thrombosis. *Arterioscler Thromb Vasc Biol.* 2012;32(3):556-562.
20. Adachi O, Kawai T, Takeda K, et al. Targeted disruption of the MyD88 gene results in loss of IL-1- and IL-18-mediated function. *Immunity.* 1998;9(1):143-150.
21. Poltorak A, He X, Smirnova I, et al. Defective LPS signaling in C3H/HeJ and C57BL/10ScCr mice: mutations in Tlr4 gene. *Science.* 1998;282(5396):2085-2088.
22. Werts C, Tapping RI, Mathison JC, et al. Leptospiral lipopolysaccharide activates cells through a TLR2-dependent mechanism. *Nat Immunol.* 2001;2(4):346-352.
23. Liliensiek B, Weigand MA, Bierhaus A, et al. Receptor for advanced glycation end products (RAGE) regulates sepsis but not the adaptive immune response. *J Clin Invest.* 2004;113(11):1641-1650.
24. Calogero S, Grassi F, Aguzzi A, et al. The lack of chromosomal protein Hmg1 does not disrupt cell growth but causes lethal hypoglycaemia in newborn mice. *Nat Genet.* 1999;22(3):276-280.
25. Faust N, Varas F, Kelly LM, Heck S, Graf T. Insertion of enhanced green fluorescent protein into the lysozyme gene creates mice with green fluorescent granulocytes and macrophages. *Blood.* 2000;96(2):719-726.
26. Jung S, Aliberti J, Graemmel P, et al. Analysis of fractalkine receptor CX(3)CR1 function by targeted deletion and green fluorescent protein reporter gene insertion. *Mol Cell Biol.* 2000;20(11):4106-4114.
27. Massberg S, Brand K, Grüner S, et al. A critical role of platelet adhesion in the initiation of atherosclerotic lesion formation. *J Exp Med.* 2002;196(7):887-896.
28. Massberg S, Gawaz M, Grüner S, et al. A crucial role of glycoprotein VI for platelet recruitment to the injured arterial wall in vivo. *J Exp Med.* 2003;197(1):41-49.
29. Altschuh D, Björkelund H, Strandgård J, Choulier L, Malmqvist M, Andersson K. Deciphering complex protein interaction kinetics using Interaction Map. *Biochem Biophys Res Commun.* 2012;428(1):74-79.
30. Urtz N, Gaertner F, von Bruehl ML, et al. Sphingosine 1-phosphate produced by sphingosine kinase 2 intrinsically controls platelet aggregation in vitro and in vivo. *Circ Res.* 2015;117(4):376-387.
31. Antoine DJ, Jenkins RE, Dear JW, et al. Molecular forms of HMGB1 and keratin-18 as mechanistic biomarkers for mode of cell death and prognosis during clinical acetaminophen hepatotoxicity. *J Hepatol.* 2012;56(5):1070-1079.
32. Liesz A, Dalpke A, Mracsko E, et al. DAMP signaling is a key pathway inducing immune modulation after brain injury. *J Neurosci.* 2015;35(2):583-598.
33. Sitia G, Iannacone M, Müller S, Bianchi ME, Guidotti LG. Treatment with HMGB1 inhibitors diminishes CTL-induced liver disease in HBV transgenic mice. *J Leukoc Biol.* 2007;81(1):100-107.
34. Ahrens I, Chen YC, Topcic D, et al. HMGB1 binds to activated platelets via the receptor for advanced glycation end products and is present in platelet rich human coronary artery thrombi. *Thromb Haemost.* 2015;114(5):994-1003.
35. Maugeri N, Rovere-Querini P, Baldini M, et al. Oxidative stress elicits platelet/leukocyte inflammatory interactions via HMGB1: a candidate for microvessel injury in sytemic sclerosis. *Antioxid Redox Signal.* 2014;20(7):1060-1074.
36. Semeraro F, Ammollo CT, Morrissey JH, et al. Extracellular histones promote thrombin generation through platelet-dependent mechanisms: involvement of platelet TLR2 and TLR4. *Blood.* 2011;118(7):1952-1961.
37. Park JS, Svetkauskaite D, He Q, et al. Involvement of toll-like receptors 2 and 4 in cellular activation by high mobility group box 1 protein. *J Biol Chem.* 2004;279(9):7370-7377.
38. Jhun J, Lee S, Kim H, et al. HMGB1/RAGE induces IL-17 expression to exaggerate inflammation in peripheral blood cells of hepatitis B patients. *J Transl Med.* 2015;13(1):310.
39. Tsung A, Tohme S, Billiar TR. High-mobility group box-1 in sterile inflammation. *J Intern Med.* 2014;276(5):425-443.
40. Sakaguchi M, Murata H, Yamamoto K, et al. TIRAP, an adaptor protein for TLR2/4, transduces a signal from RAGE phosphorylated upon ligand binding. *PLoS One.* 2011;6(8):e23132.
41. Medzhitov R, Preston-Hurlburt P, Kopp E, et al. MyD88 is an adaptor protein in the hToll/IL-1 receptor family signaling pathways. *Mol Cell.* 1998;2(2):253-258.
42. Myers DD Jr, Rectenwald JE, Bedard PW, et al. Decreased venous thrombosis with an oral inhibitor of P selectin. *J Vasc Surg.* 2005;42(2):329-336.
43. Myers DD Jr, Wrobleski SK, Longo C, et al. Resolution of venous thrombosis using a novel oral small-molecule inhibitor of P-selectin (PSI-697) without anticoagulation. *Thromb Haemost.* 2007;97(3):400-407.
44. Brinkmann V, Reichard U, Goosmann C, et al. Neutrophil extracellular traps kill bacteria. *Science.* 2004;303(5663):1532-1535.
45. Fuchs TA, Brill A, Duerschmied D, et al. Extracellular DNA traps promote thrombosis. *Proc Natl Acad Sci USA.* 2010;107(36):15880-15885.
46. Mangold A, Alias S, Scherz T, et al. Coronary neutrophil extracellular trap burden and deoxyribonuclease activity in ST-elevation acute coronary syndrome are predictors of ST-segment resolution and infarct size. *Circ Res.* 2015;116(7):1182-1192.
47. Massberg S, Grahl L, von Bruehl ML, et al. Reciprocal coupling of coagulation and innate immunity via neutrophil serine proteases. *Nat Med.* 2010;16(8):887-896.
48. Rouhiainen A, Imai S, Rauvala H, Parkkinen J. Occurrence of amphoterin (HMG1) as an endogenous protein of human platelets that is exported to the cell surface upon platelet activation. *Thromb Haemost.* 2000;84(6):1087-1094.
49. Yang X, Wang H, Zhang M, Liu J, Lv B, Chen F. HMGB1: a novel protein that induced platelets active and aggregation via Toll-like receptor-4, NF-κB and cGMP dependent mechanisms. *Diagn Pathol.* 2015;10:134.
50. Ito T, Kawahara K, Nakamura T, et al. High-mobility group box 1 protein promotes development of microvascular thrombosis in rats. *J Thromb Haemost.* 2007;5(1):109-116.
51. Andrassy M, Volz HC, Igwe JC, et al. High-mobility group box-1 in ischemia-reperfusion injury of the heart. *Circulation.* 2008;117(25):3216-3226.
52. Tsung A, Klune JR, Zhang X, et al. HMGB1 release induced by liver ischemia involves Toll-like receptor 4 dependent reactive oxygen species production and calcium-mediated signaling. *J Exp Med.* 2007;204(12):2913-2923.
53. Tsung A, Sahai R, Tanaka H, et al. The nuclear factor HMGB1 mediates hepatic injury after murine liver ischemia-reperfusion. *J Exp Med.* 2005;201(7):1135-1143.
54. Dewyer NA, El-Sayed OM, Luke CE, et al. Divergent effects of Tlr9 deletion in experimental late venous thrombosis resolution and vein wall injury. *Thromb Haemost.* 2015;114(5):1028-1037.

55. Huebener P, Pradere JP, Hernandez C, et al. The HMGB1/RAGE axis triggers neutrophil-mediated injury amplification following necrosis. *J Clin Invest.* 2015;125(2):539-550.

56. Schiraldi M, Raucci A, Muñoz LM, et al. HMGB1 promotes recruitment of inflammatory cells to damaged tissues by forming a complex with CXCL12 and signaling via CXCR4. *J Exp Med.* 2012;209(3):551-563.

57. Zandarashvili L, Sahu D, Lee K, et al. Real-time kinetics of high-mobility group box 1 (HMGB1) oxidation in extracellular fluids studied by in situ protein NMR spectroscopy. *J Biol Chem.* 2013; 288(17):11621-11627.

58. LeBlanc PM, Doggett TA, Choi J, et al. An immunogenic peptide in the A-box of HMGB1 protein reverses apoptosis-induced tolerance through RAGE receptor. *J Biol Chem.* 2014; 289(11):7777-7786.

59. Hori O, Brett J, Slattery T, et al. The receptor for advanced glycation end products (RAGE) is a cellular binding site for amphoterin. Mediation of neurite outgrowth and co-expression of rage and amphoterin in the developing nervous system. *J Biol Chem.* 1995;270(43):25752-25761.

60. Huttunen HJ, Fages C, Kuja-Panula J, Ridley AJ, Rauvala H. Receptor for advanced glycation end products-binding COOH-terminal motif of amphoterin inhibits invasive migration and metastasis. *Cancer Res.* 2002;62(16):4805-4811.

61. Rauvala H, Rouhiainen A. Physiological and pathophysiological outcomes of the interactions of HMGB1 with cell surface receptors. *Biochim Biophys Acta.* 2010;1799(1-2):164-170.

62. Mitroulis I, Kambas K, Chrysanthopoulou A, et al. Neutrophil extracellular trap formation is associated with IL-1β and autophagy-related signaling in gout. *PLoS One.* 2011;6(12):e29318.

63. Renné T, Pozgajová M, Grüner S, et al. Defective thrombus formation in mice lacking coagulation factor XII. *J Exp Med.* 2005;202(2):271-281.

64. Rouhiainen A, Kuja-Panula J, Wilkman E, et al. Regulation of monocyte migration by amphoterin (HMGB1). *Blood.* 2004;104(4):1174-1182.

65. Li L, Ling Y, Huang M, et al. Heparin inhibits the inflammatory response induced by LPS and HMGB1 by blocking the binding of HMGB1 to the surface of macrophages. *Cytokine.* 2015;72(1): 36-42.

66. Hou CH, Fong YC, Tang CH. HMGB-1 induces IL-6 production in human synovial fibroblasts through c-Src, Akt and NF-κB pathways. *J Cell Physiol.* 2011;226(8):2006-2015.

67. Li J, Kokkola R, Tabibzadeh S, et al. Structural basis for the proinflammatory cytokine activity of high mobility group box 1. *Mol Med.* 2003;9(1-2): 37-45.

68. Kanellakis P, Agrotis A, Kyaw TS, et al. High-mobility group box protein 1 neutralization reduces development of diet-induced atherosclerosis in apolipoprotein e-deficient mice. *Arterioscler Thromb Vasc Biol.* 2011;31(2): 313-319.

69. Kokkola R, Li J, Sundberg E, et al. Successful treatment of collagen-induced arthritis in mice and rats by targeting extracellular high mobility group box chromosomal protein 1 activity. *Arthritis Rheum.* 2003;48(7):2052-2058.

2016 128: 2435-2449
doi:10.1182/blood-2016-04-710632 originally published online August 29, 2016

Disulfide HMGB1 derived from platelets coordinates venous thrombosis in mice

Konstantin Stark, Vanessa Philippi, Sven Stockhausen, Johanna Busse, Antonella Antonelli, Meike Miller, Irene Schubert, Parandis Hoseinpour, Sue Chandraratne, Marie-Luise von Brühl, Florian Gaertner, Michael Lorenz, Alessandra Agresti, Raffaele Coletti, Daniel J. Antoine, Ralf Heermann, Kirsten Jung, Sven Reese, Iina Laitinen, Markus Schwaiger, Axel Walch, Markus Sperandio, Peter P. Nawroth, Christoph Reinhardt, Sven Jäckel, Marco E. Bianchi and Steffen Massberg

Blood (print ISSN 0006-4971, online ISSN 1528-0020), is published weekly by the American Society of Hematology, 2021 L St, NW, Suite 900, Washington DC 20036.